Earth and Planetary Science Letters 310 (2011) 327–333

Contents lists available at SciVerse ScienceDirect

Earth and Planetary Science Letters

journal homepage: www.elsevier.com/locate/epsl

Geological evidence for a migrating Tharsis plume on early Mars

Brian M. Hynek [a,b,*], Stuart J. Robbins [b,c], Ondřej Šrámek [d], Shijie J. Zhong [d]

[a] Department of Geological Sciences, 399 UCB, University of Colorado, Boulder, CO 80309, United States
[b] Laboratory for Atmospheric and Space Physics, 392 UCB, University of Colorado, Boulder, CO 80309, United States
[c] Department of Astrophysical and Planetary Sciences, 391 UCB, University of Colorado, Boulder, CO 80309, United States
[d] Department of Physics, 390 UCB, University of Colorado, Boulder, Colorado, CO 80309, United States

ARTICLE INFO

Article history:
Received 8 January 2011
Received in revised form 11 August 2011
Accepted 11 August 2011
Available online xxxx

Editor: T. Spohn

Keywords:
Mars
Tharsis
mantle plume
geodynamics
geology
impact craters

ABSTRACT

The Tharsis bulge is the largest magmatic/volcanic center on Mars and in the solar system, having a volume of ~3×10^8 km^3, with the majority of its mass emplaced more than 3.7 billion years ago. The igneous history of Tharsis has been implicated in the generation of an atmosphere and hydrosphere capable of clement conditions on early Mars. It has been proposed that an early plume migration from the southern highlands of Mars relative to a one-plate lithosphere led to the development of the Tharsis bulge in its current location along the Martian crustal dichotomy. We used geologic mapping, crustal magnetic data, crater age-dating and crater morphometry to detail a previously-unidentified path of putative plume migration. Our results indicate that extensive volcanic resurfacing occurred from a location near the present south pole to the equator around 3.8 billion years ago, obliterating older cratered terrains. The resurfacing path is manifest as smooth volcanic plains embaying ancient massifs and infilling large impact craters as well as a lack of a magnetic signature in this portion of the crust. Our results have significant ramifications for mantle dynamics and the early geologic history of Mars.

1. Introduction

Volcanoes in the Tharsis region of Mars were first identified from the Mariner spacecraft images returned in the late 1960s (e.g. Carr, 1974), and they have since gained recognition as the largest volcanoes in the solar system. However, it was not until topographic information was returned from the Mars Global Surveyor mission (Smith et al. 2001) that the extent of the massive Tharsis bulge was revealed. This feature covers one-quarter of the planet and has had a profound effect on the long-wavelength topography and gravity signatures of Mars (Phillips et al., 2001). Tharsis is centered approximately at the boundary of the crustal dichotomy, which is another tectonic and topographic feature of a hemispheric scale. The extensive igneous activity of Tharsis is thought to be a result of mantle plume upwellings and decompression melting (e.g., Mège and Masson, 1996). Mapping of associated tectonic structures (Anderson et al., 2001) and dried river valley azimuths (Phillips et al., 2001) suggest most of the load was emplaced in the Noachian epoch, prior to ~3.7 Ga, although surface lava flows continued to form on some volcanic constructs until a few million years ago (Hartmann, 1999; Robbins et al., 2010). Numerous models for the development of Tharsis have been proposed, including mantle plumes (Breuer et al., 1996; Carr, 1974; Harder and Christensen, 1996; Kiefer and Hager, 1989; Li and Kiefer, 2007; Mège and Masson, 1996; Roberts and Zhong, 2004; Wenzel et al., 2004; Zhong, 2009) and igneous intrusion into and extrusions atop a thin, weak lithosphere overlying an anomalously warm mantle (Solomon and Head, 1982).

Wenzel et al. (2004) and Zhong (2009) explored possible dynamic links between Tharsis and the crustal dichotomy. Wenzel et al. (2004) showed that the thickened crust in the southern highlands would induce mantle upwelling plumes beneath the thickened crust due to its insulation effects. However, Wenzel et al. (2004) could not explain the equatorial location of Tharsis. Zhong (2009), on the other hand, favored a Tharsis mantle plume source that formed and migrated under a lithospheric keel and the thickened crust from the southern highlands to the crustal dichotomy boundary. Spherical shell models of mantle convection on a one-plate planet were used to demonstrate that a unique mode of horizontal motion (rotation) of the entire one-plate lithosphere with respect to the underlying mantle, is readily excited for Mars by one-plume convection in the presence of lithospheric thickness variations (Šrámek and Zhong, 2010; Zhong, 2009). This causes relative motion of the plume with respect to the lithosphere, or apparent plume migration. The suggested mechanism explains the temporal and spatial patterns of Tharsis volcanism – in particular the apparent migration of the Tharsis volcanic center from southern latitudes (e.g., Thaumasia region) to the dichotomy boundary in the Noachian (Anderson et al., 2001; Frey, 1979; Johnson and Phillips,

* Corresponding author at: LASP/University of Colorado, 392 UCB, Boulder, CO 80309, USA. Tel.: +1 303 735 4312.
E-mail address: hynek@lasp.colorado.edu (B.M. Hynek).

0012-821X/$ – see front matter
doi:10.1016/j.epsl.2011.08.020

2005; Mège and Masson, 1996) – and offers a path to a unified model for the Tharsis bulge and the crustal dichotomy.

In this model (Zhong, 2009), the lithosphere in the southern highlands is assumed to be significantly thicker than near its equatorial margins (i.e. lithosphere keel), consistent with estimates for contemporary crustal thickness of the ancient highlands (Zuber, 2000), assuming that the thickened crust formed by partial melting of the underlying mantle; the keel thus represents the stiff (devolatilized) melt residue. Spherical shell models of mantle convection (Zhong, 2009) demonstrate that the lithospheric keel causes the one-plume upwelling structure to form below the keel (Fig. 1a). However, this configuration is dynamically unstable, causing relative motion of the plume with respect to the lithospheric keel and apparent plume migration as well as stretching of the upwelling structure into an elongated, ridge-like shape (Fig. 1b). The relative motion of the plume with respect to the lithosphere wanes after the plume reaches the crustal dichotomy boundary where the original crust, hence the lithosphere, is thin (Fig. 1c). Depending on inputs for mantle viscosity structures and lithospheric keel thickness, the relative motion of the plume with respect to the lithosphere ranges from 0.2°/Ma to 1.5°/Ma (Šrámek and Zhong, 2010; Zhong, 2009). We would like to point out that in a physically reasonable no-net rotation mantle reference frame, the lithospheric shell has a significantly larger rotation motions than the underlying mantle and mantle plumes (Zhong, 2009), and that our discussions in this paper emphasize the relative motions between the lithosphere and mantle.

This plume model is only one of many hypotheses for Tharsis formation, yet it has specific predictions about melting and surface volcanism (Zhong, 2009). No significant melting is expected from the plume initially when the plume is below the center of the lithospheric keel (near the modern south pole) because the thick keel prevents the plume from rising to shallow depths (Fig. 1a). However, as the plume moves away from the center of the keel, it may rise to shallower depths to initiate melting and volcanism at the surface (Fig. 1 b–c). The initial phase of melting and volcanism could be rather moderate, depending on the lithosphere thickness. However, when the plume moves toward the crustal dichotomy boundary where the lithosphere is thin, extensive melting occurs and gives rise to the Tharsis bulge (Fig. 1c). The goal of this study is to test this plume migration model by using geologic mapping, crustal magnetic data, crater age-dating and crater morphometry in the southern highlands of Mars.

2. Methods and results

To test the migrating plume/rotating keel model, we completed geologic mapping, analyzed impact craters (Robbins and Hynek, 2010) and structural features, and used the remnant crustal magnetization (Whaler and Purucker, 2005) in the region south of the Tharsis bulge to investigate any potential crustal signatures of plume migration through this area during the Noachian epoch (Fig. 2). Geologic mapping of the region south of the entire Tharsis bulge (roughly one-third of the planet south of 40°S, totaling 5.6×10^7 km^2 in area) was completed at ~1:5,000,000-scale and we identified seven major units on the basis of morphology and topography (Fig. 2). We used topography from the Mars Global Surveyor (Smith et al. 2001) and visible images combined with a global daytime thermal infrared mosaic (Christensen et al., 2004) to delineate major geologic units south of the Tharsis bulge (Fig. 2a). Two types of cratered highlands are present — ancient, rugged massifs (cratered unit) and a subdued cratered unit that is still heavily cratered but the craters are infilled and with subdued rims, indicative of significant fluvial erosion in the Noachian (Craddock and Howard, 2002). The Thaumasia highland volcanic terrain was delineated and contains some of the oldest Tharsis materials (Anderson et al., 2001; Dohm et al., 2001; Johnson and Phillips, 2005). The south polar cap and associated deposits were mapped as one unit. The associated surrounding deposits are plains inferred to be resurfaced materials likely from the advance and retreat of the ice cap and contain topographically low plains with eskers and other diagnostic features of glacial activity (Head and Pratt, 2001). The crater unit contains two very large, young, and fresh impact craters, including Lowell, which superpose all other units and were excluded from the analysis to prevent their local resurfacing from affecting crater statistics. Two plains units are also present — low-lying, aligned smooth units and smaller, ridged plains that occur as isolated exposures throughout the southern highlands of Mars (similar to unit Hr on the global maps of Scott and Tanaka (1986) and Greeley and Guest (1987)).

The geographically extensive and aligned plain unit boundaries correlate well with smooth terrains from Scott and Tanaka (1986), although they distinguished four units whereas we grouped these together based on consistent morphology, topographic expression, texture, and embayment relationships throughout the region (Fig. 3). Specifically, the southernmost smooth plains unit we map corresponds to the Dorsa Argentea Formation, lower member (Scott and Tanaka, 1986), which is also prevalent around the south polar cap and extending north along the prime meridian to 60°S (Fig. 2b). We separated the southern plain unit from the rest of the Dorsa Argentea Formation unit on the basis of different expression, including the less rugged topography of the plain unit, the lack of chaotic/differentially eroded terrains that occur on the more southern units, and lack of eskers or periglacial features that are characteristic of this member. The central part of the plain unit correlates with an Npl2 unit from Scott and Tanaka (1986). While a number of other Npl2 units are prevalent in the region (particularly to the west) this unit has a much different character, including an expression of smooth plains with a dearth of craters (Fig. 2). Finally, the northernmost plain unit corresponds well with an Hpl3 unit —

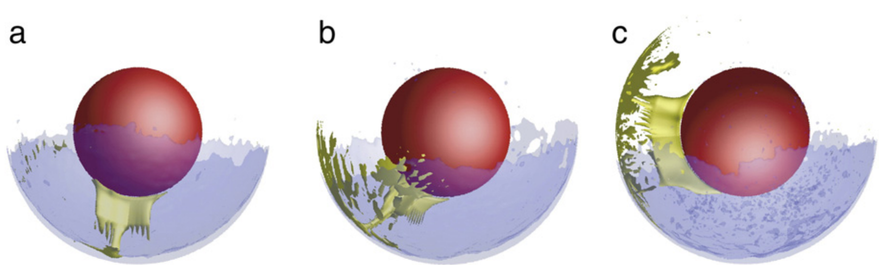

Fig. 1. Three time-series snapshots from the 3-D spherical shell convection model, modified from Zhong (2009). The transparent blue isosurface shows the lithospheric keel of roughly hemispheric extent, assumed to represent the high-viscosity melt residue left after the formation of the thicker southern highlands crust by partial melting. In yellow is the positive thermal anomaly which shows as a single upwelling. This upwelling initially forms below the center of the southern highlands (a) and subsequently migrates towards the edge of the thickened lithosphere, i.e. the dichotomy boundary (b). The upwelling then remains centered near the dichotomy boundary and at depth assumes an elongated, ridge-like shape perpendicular to the boundary due to shear stresses, from which several individual plumes may rise to the surface (c). These plumes caused extended volcanism along the original plume track and significantly more melt is present as the plume reaches the edge of the keel. The figure is presented with the lithosphere fixed to highlight the relative motions between the lithosphere and mantle plume. In a no-net rotation mantle reference frame, the lithospheric shell has a significantly larger rotation motion than the underlying mantle (Zhong, 2009).

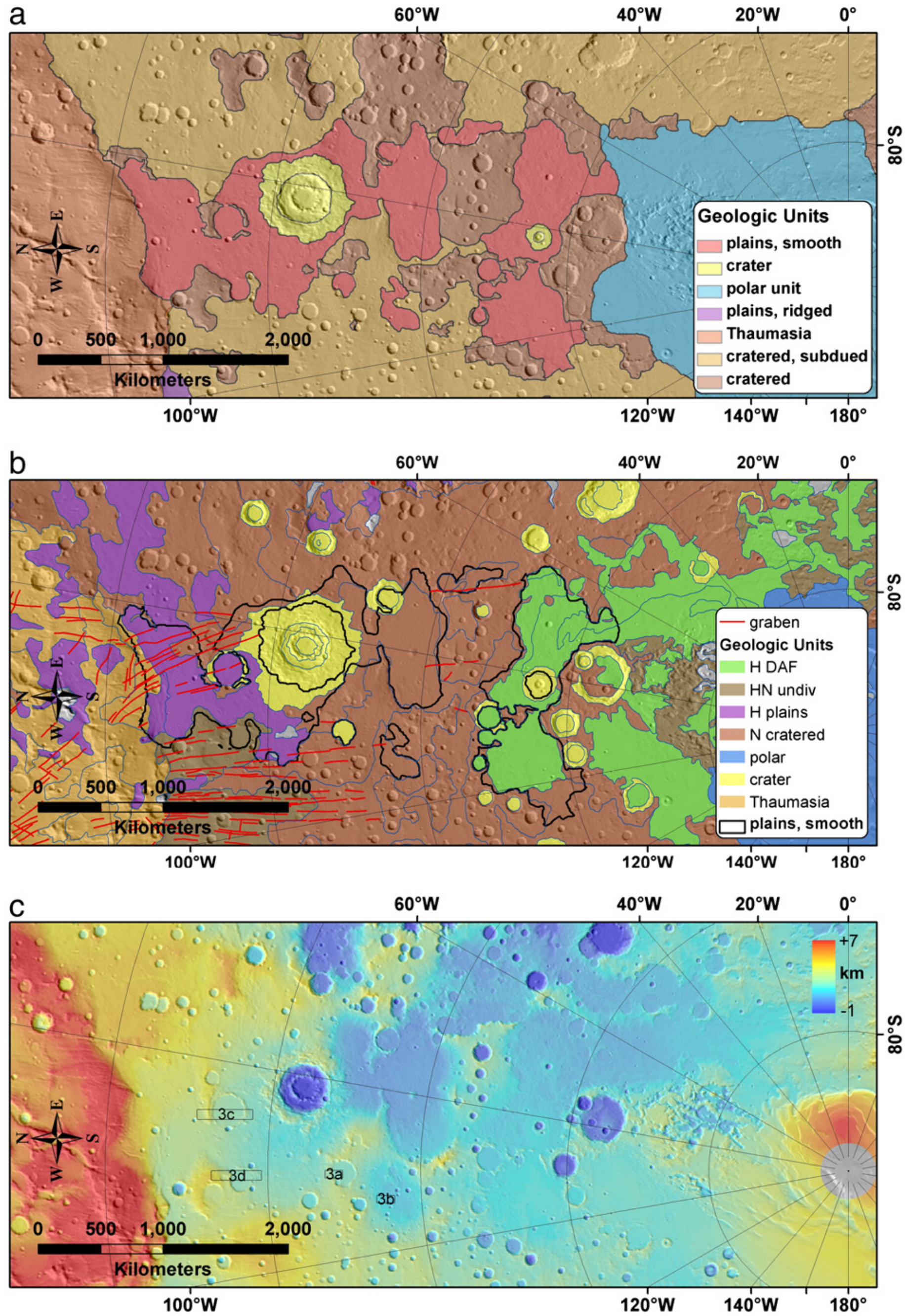

Fig. 2. Putative Tharsis plume track (smooth plain unit). (a) Geologic map of materials south of the ancient Tharsis massif of Thaumasia. (b) Geologic map for comparison from Scott and Tanaka (1986). Units have been appropriately grouped but original unit contacts are shown in blue. Our mapping is consistent with previous work although different groupings are noted in the text. Red lines show major extensional structures that formed in the Late Noachian/Early Hesperian (from Scott and Tanaka, 1986; Dohm et al., 2001) (c) MOLA topography of region (Smith et al. 2001) and low-lying areas embaying older cratered terrains correspond to smooth plain unit from (a). Index boxes for Figs. 3 a–d are noted.

plateau sequence from Scott and Tanaka (1986). North of these aligned plains units lie the Thaumasia Highlands, that are thought to be an early focus of Tharsis activity (e.g. Dohm and Tanaka, 1999). Our smooth plain unit is also consistent with mapping by Tanaka and Kolb (2001), who considered much of this unit to be the Dorsa Argentea Formation. Volume arguments of these plains led the workers to hypothesize that there was potentially a deep-seated magma source that led to extensive surface volcanic activity, but they note “the lack of large associated volcanic collapse structures is problematic, unless the magmas arose straight from great depths and did not reside in shallow chambers.” Instead, the workers favored an interpretation of debris flows; however, the source and mechanism remain a mystery.

The prevalent smooth plains units between Thaumasia and the south polar ice cap embay heavily cratered ancient highland inliers (Fig. 2). These plains have lobate margins, constant and low elevation surfaces, onlap relationships with surrounding higher-standing older units, evidence for overtopping and infilling of large impact basins, and morphologies consistent with low-viscosity volcanic extrusions (Fig. 3). Large craters are infilled with smooth plains and older rugged mountain regions are embayed by similar materials (Figs. 3 c–d). Given these characteristics, we infer that the plains formed by flood volcanism.

Are these aligned and geographically extensive plains units unique to the southern highlands? It is beyond the scope of this

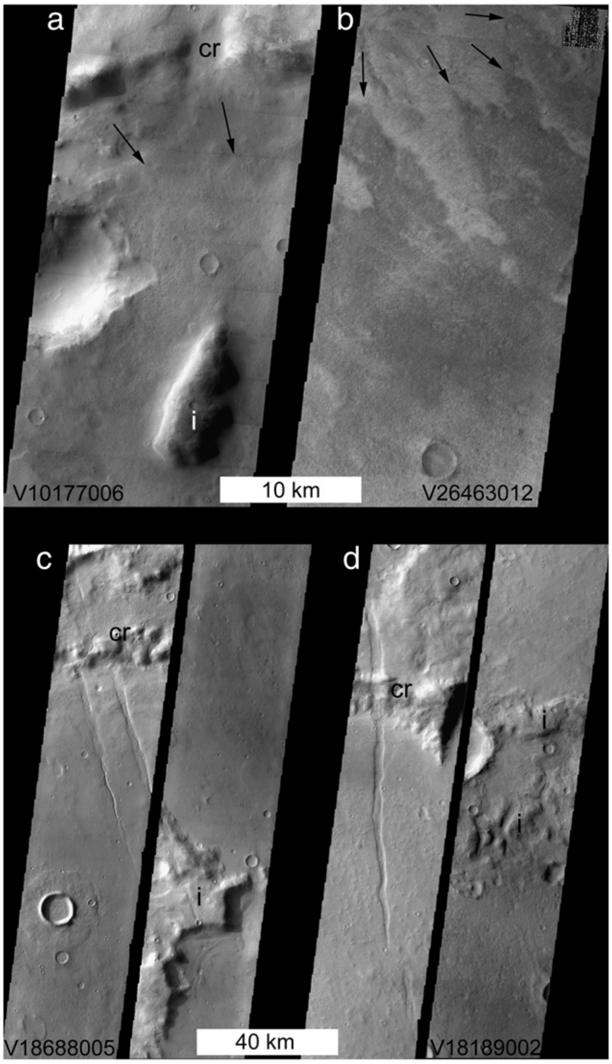

Fig. 3. Photogeologic documentation with THEMIS visible images (Christensen et al., 2004) of the smooth plain unit, inferred to be the plume track. Lobate margins are noted (arrows) as are the onlapping and embayment relations of older inliers (i) and large crater rims (cr). The smooth plains have a consistent character across the images.

paper to remap the entire southern hemisphere of Mars, but inspection of the existing global maps (Greeley and Guest, 1987; Scott and Tanaka, 1986) and southern hemisphere of Tanaka and Kolb (2001) show that a similar linear trend of plains units does not exist elsewhere in the southern hemisphere. The rest of the Dorsa Argentea Formation is distinctly different than the units included in the smooth plain boundaries: they consist of pitted, hummocky and rugged terrains and often have long curvilinear ridges interpreted as eskers. This description characterizes the large Dorsa Argentea units to the east of the putative plume track. Other smooth plains units occasionally occur within the southern highlands (often correlating with unit Hr from Scott and Tanaka (1986) and Greeley and Guest (1987)), they are much smaller in area, show a more random distribution, and are not spatially aligned like those found in this region. In terms of area, the only substantial smooth plains (unit Hr from Greeley and Guest, 1987) are directly south of Amphrites, Pityusa, and Malea Paterae, low-relief Noachian-age calderas southeast of the Hellas Basin. We infer these smooth plains also consist of volcanically resurfaced terrains related to the local volcanoes. Finally, the smooth plains units south of Thaumasia show a dearth of larger impact craters (>15-km-diameter). The size-frequency distribution (SFD) of craters is another way to assess the possibility of other similar units in the southern highlands. As shown in Fig. 4a, the only other terrains showing a lack of larger craters are directly within and southeast of the southern Hellas paterae mentioned above. Thus, we conclude that no other portion in the southern highlands has any smooth plains of similar spatial extent or arrangement in a linear pattern spanning ~2000 km.

Crater age determinations were completed on all geologic units in the region. We used a global crater database (Robbins and Hynek, 2010) that contains ~631,333 impact craters and is statistically complete to ~1-km-diameter to conduct crater counts on all units (Fig. 5). We binned the craters at $^{8}\sqrt{2}D$, which is a finer diameter binning than typical, but provides a more continuous curve that is well-suited for characterizing resurfacing events. The cratering absolute chronology is from Hartmann and Neukum (2001) and the crater production function and polynomial coefficients of Ivanov (2001) were used to estimate absolute ages. Error bars were calculated by standard $\pm\sqrt{N}$ Poisson statistics (Arvidson et al., 1979). These are the formal errors, but greater uncertainty likely exists given the uncertainties of crater-age dating on planets without samples from known locations. The cratered highlands date to >3.90 Ga, as does the Thaumasia unit that represents some of the earliest volcanism on the Tharsis bulge (Anderson et al., 2001; Dohm et al., 2001) (Fig. 5). The plain unit representing the surface signature of the inferred plume dates to a similar age when using craters larger than ~65-km-diameter, mimicking that of other cratered units. Between 65 and 20 km diameter, there is a downturn in the slope of the crater SFD (Fig. 5). This can most easily be explained by a significant resurfacing event that removed all craters smaller than 65 km around 3.8 Ga and then subsequent crater production on the new surface at smaller diameters has occurred since 3.52 Ga. These two surface age estimates from the smooth plains unit effectively bracket the timing of plume migration and finality of surface volcanism in the region. Indeed, a map of all craters >15-km-diameter (Robbins and Hynek, 2010) shows a low density region that corresponds with the putative plume track (Fig. 4a). This is in contrast with the rest of the global southern highlands, which show densities similar to the cratered units seen in Figs. 2 and 4.

We find that the average crater depth in the putative plume track is significantly shallower than in the cratered unit for diameters $D>50$ km and is also much shallower than in the subdued unit for $50<D<70$ km. In fact, the mean depth of the smooth plains units' craters in the 50–100 km range is 0.37 km ($N=13$; $1\sigma=0.20$) while the average depth of equivalent craters in the cratered unit is 1.37 km ($N=58$; $1\sigma=0.62$). Additionally, rim heights in the plain unit are a factor of two shallower than those in the adjacent Noachian cratered unit. Collectively, these results are indicative of extensive, presumably volcanic, infilling of the plain unit's larger craters. The cratered unit appears to be a good representation of the southern hemisphere in terms of crater depth versus diameter (Robbins and Hynek, 2010), so it is a fair comparison to make and provides additional support that the plain unit is unique in the southern highlands.

Mars has remnant crustal magnetization across much of the southern highlands created by thermal magnetization from an active dynamo and igneous processes in the crust (Connerney et al., 2001; Lillis et al., 2004; Nimmo and Tanaka, 2005; Whaler and Purucker, 2005). The dynamo is thought to have operated prior to 4.0 Ga, since large impact basins, including Argyre Basin, that formed since that time contain no magnetic signature (Nimmo and Tanaka, 2005). The inferred plume track geographically correlates to crust with little to no detected magnetic signature while surrounding units, and most of the southern highlands, are magnetized (Fig. 4b). We argue that plume-related volcanism effectively removed any previous crustal magnetic signature in this area as it migrated through the region after the dynamo shut down. Additionally, plume tracks are typically associated with a thickened crust, owing in part to significant intrusive and extrusive activity. Cheung and King (2011)

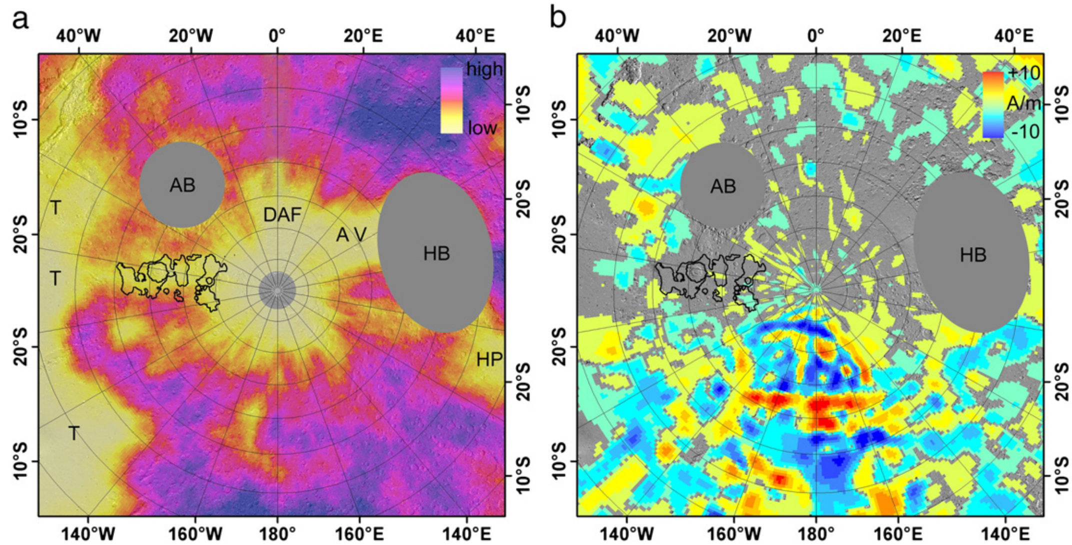

Fig. 4. (a) Crater density of all craters with diameters >15 km and smooth plains unit from Fig. 2a (black outlines). (b) Radial component of remnant crustal magnetization at the surface (Whaler and Purucker, 2001) and putative plume track (black outlines). AB = Argyre Basin, HB = Hellas Basin, AV = Amphrites Volcanics, HP = Hesperia Planum volcanics, T = Tharsis volcanics, DAF = Dorsa Argentea Formation.

reported a relatively thickened crust that spatially correlates with the path of our inferred plume migration through the southern hemisphere.

A large amount of Tharsis plume migration should be accommodated by large extensional strain near the track of the plume. Such a notion has predictable consequences, as demonstrated by Grimm and Solomon (1986). Specifically the workers predict that paleopole rotation should be accommodated by large extensional strain adjacent to the track of true polar wander. In fact, there are large graben systems adjacent to both sides of the smooth plain unit (Fig. 2b) that date to the Late Noachian or Early Hesperian (Anderson et al., 2001; Dohm et al., 2001). Detailed mapping by Dohm and Tanaka (1999) indicates a sharp decline of normal faulting in the Early to Late Hesperian. The southern extent of the plume track has relatively few faults, but more than the rest of high southern latitudes. Yet moving northward, toward a thinner lithosphere, the extensional tectonic expression is more pervasive (Figs. 2b, 3c–d). Some of these are likely due to radial extensional stresses from the Warrego and Claritas Rises; however, their great southward extension beyond these regions (>1000 km) is problematic for their relation to these rises

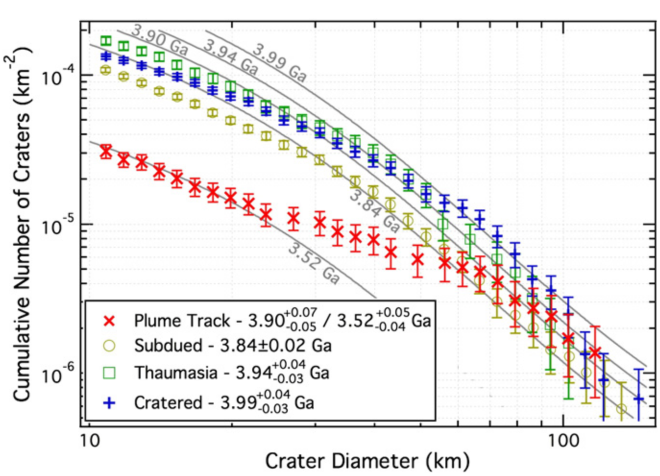

Fig. 5. Crater size-frequency distributions of selected geologic units identified from mapping. Note the downturn of the smooth plains (plume track) unit starting at ~65 km to smaller diameters. Age determinations and error bars are described in the Methods section.

(J. Dohm, personal communication). Our model of plume migration and true polar wander in this region provides an explanation for these extensional features well south of the Tharsis region.

3. Discussion

Collectively, the geologic mapping, crater analysis, and lack of a magnetic signature are consistent with migration of a mantle plume below the Martian lithosphere shell, and we now develop a conceptual model to support the observations. Between 3.9–3.5 Ga, a mantle plume migrated under the lithospheric keel from near the present south pole (i.e. the center of the thickened crust and highlands), roughly along the 85°W meridian, to the geographic center of the Thaumasia region. Model calculations indicate that this process took 33–250 Ma (Šrámek and Zhong, 2010). The surface manifestation consisted of significant flood volcanism seen today as the plume track's smooth plains, which embayed surrounding cratered highland terrains and impact craters and also obliterated craters <65-km-diameter. We estimate that the surface flood lavas are on average ~2.5–3 km thick, given that they infilled craters <65 km, and the depth-to-diameter ratio for the freshest present-day Martian complex craters in that size range is about 1 to 20–25 (Robbins and Hynek, 2010). This explains the old age of the plume track's surface at large crater diameters and the downturn in the crater SFD at diameters <65 km (Fig. 5). This depth of infilling is slightly larger than the thickest parts of the Deccan Traps (Singhal, 1997) for a plume track that is roughly six times as wide as the Yellowstone Hotspot as it moved through the Snake River Plains in Idaho, USA. The surface signature of this latter terrestrial example also includes smooth low-lying plains that embay older crustal materials. In both cases, the plume-related surface flood volcanism was likely accompanied by significant intrusive magmatism in the crust (e.g. Mège and Masson, 1996; Šrámek and Zhong, 2010). The thermal effect of the combined magmatic activity erased the magnetic signature of the crust; a total accumulated magma thickness necessary to demagnetize the crust was estimated by Lillis et al. (2009) to be 1 to a few tens of kilometers.

The youthfulness of the Tharsis plume unit's surface age relative to the Thaumasia igneous center at smaller crater diameters (Fig. 5) (roughly 300 million years younger) can be attributed to residual melt and volcanism from decompression melting as the plume moved northward and uplift of the ancient Thaumasia highlands. Fig. 1 shows that during migration from the center of the lithospheric keel, shear stresses cause the plume at depth to assume an elongated, ridge-like shape perpendicular to the dichotomy boundary from which several individual plumes may rise to the surface, causing long-lived volcanism along the plume track, possibly simultaneous at different locations (Fig. 1 b–c). As a result, the surface plume track may show a discontinuous spatial pattern, and may not necessarily exhibit a clear along-track age progression. The plume volcanism is manifest in the aligned plains unit as a downturn in its SFD of craters around 65 km (Fig. 5). Finally, large and extensive grabens are noted flanking the plume track and this is consistent with plume migration relative to the lithosphere.

The Thaumasia highlands represent an uplifted and partially resurfaced region evident from pervasive tectonic deformation (Dohm et al., 2001) and in some places the retention of remnant crustal magnetization (Whaler and Purucker, 2005). We infer that plume migration toward the thinner edge of the lithospheric keel in this region is the mechanism for uplift and resulted in the cratered, tectonically deformed and volcanically modified highland terrain present today. In this case, Thaumasia is a spatial gap of extensive surface activity due to the locally thick crust that underwent uplift. However, the density of large craters is still diminished in this region (Fig. 4a), indicating at least some surface volcanism. The 5-km-relief Warrego Rise in Thaumasia has been attributed to potential plume activity or mantle underplating (Dohm and Tanaka, 1999). These workers noted 14 mountainous rises in this region, many of which have summit pits. They argued that these features are likely ancient volcanic constructs, although no source mechanism has been noted for extensive magmatism in this location. Some of these rises are immediately northwest of Warrego and are also attributed to extensive uplift and extrusive volcanism (Dohm and Tanaka, 1999). We hypothesize that once it reached the Thaumasia highlands, the plume migrated to the northwest, uplifting that portion of the plateau and causing extensive volcanism beyond the uplifted block. Past this time marker, the plume track is lost, owing to extensive younger volcanic resurfacing of much of the Tharsis rise.

The most well-known terrestrial example of a mantle plume migrating under a thick continental crust is the Yellowstone hotspot track (YHT). The YHT originated around 16 million years ago in the Columbia River Plateau and was coincident with the Columbia River flood basalts and neighboring dike swarms (e.g., Glen and Ponce, 2000). As the North American plate migrated northwest, flood volcanism continued, most clearly along the Snake River Plain, Idaho. The topographic expression of this activity consists of a track of low-lying and aligned smooth plains with occasional interruption by older crustal materials. While a number of silicic caldera complexes have been identified by local studies, the gross topography shows few volcanic constructs, consistent with a deep source of magmatism. As noted above, the putative Tharsis plume track shows a similar surface expression, with sub-linear, low-lying plains that inundate the existing topography and with occasional older crustal regions that lack a surface expression of volcanic constructs.

Our model of relative motion between the lithosphere shell and its underlying mantle/mantle plume may have implications for true polar wander (TPW), although they have completely different physical mechanisms, as pointed out by Zhong (2009). If the relative motion between lithosphere shell and the mantle is along an axis that differs significantly from the spin axis, then the relative motion of lithosphere shell would result in development of rotational bulge and transit of surface features (e.g., crustal magnetic anomalies) that are equivalent to those expected from TPW (Zhong, 2009). TPW on Mars has been a controversial topic. Studies on paleomagnetic poles (Arkani-Hamed and Boutin, 2004; Hood et al., 2005), deformed shorelines (Perron et al., 2007) and the moment of inertia from the Martian crust dichotomy (Roberts and Zhong, 2007) suggested significant TPW in different periods of time ranging from the pre-Noachian (i.e., formation of the crustal dichotomy) to that significantly post-dated the formation of Tharsis. However, the lack of global tectonic deformation predicted from TPW calculations (Grimm and Solomon, 1986; Melosh, 1980) and stabilizing effects of thick elastic shell on the spin axis (Willemann, 1984) were also used as evidence for little or no TPW on Mars. Yet recent theoretical work by Matsuyama et al. (2006) indicated that significant post-Tharsis TPW is possible, which provided the basis to interpret the shorelines in terms of TPW (Perron et al., 2007). Since our proposed relative motion of lithosphere shell and the mantle plume post-dates the crustal dichotomy and pre-dates the Tharsis bulge, it is possible that the variations in paleomagnetic pole locations (Arkani-Hamed and Boutin, 2004; Hood et al., 2005) may result from our proposed relative motion of lithosphere shell rather than TPW. Future studies need to examine how TPW and our proposed relative motion of lithosphere shell to the underlying mantle may manifest themselves in surface deformation.

In summary, our model provides a source and pathway for the mantle plume ultimately responsible for the formation of the Tharsis bulge. We hypothesize that starting around 3.9 billion years ago, a plume migrated approximately from near the current south pole of Mars underneath the lithospheric keel roughly 4000 km toward the crustal dichotomy boundary near the equator. This contributed significant extrusive volcanism at the surface that buried an older cratered terrain. Our results have significant implications for mantle dynamics and resultant magmatism and volcanism on ancient Mars.

Acknowledgments

This work was supported by NASA-MDAP Grant Award NNX10AL62G to BMH and NASA MFRP Grant Award NNX08AN12G to SJZ.

References

Anderson, R.C., Dohm, J.M., Golombek, M.P., Haldemann, A.F.C., Franklin, B.J., Tanaka, K.L., Lias, J., Peer, B., 2001. Primary centers and secondary concentrations of tectonic activity through time in the western hemisphere of Mars. J. Geophys. Res. 106, 20,563–20,585.

Arkani-Hamed, J., Boutin, D., 2004. Paleomagnetic poles of Mars: revisited. J. Geophys. Res. 109. doi:10.1029/2003JE002229.

Arvidson, R., Boyce, J., Chapman, C., Cintala, M., Fulchignoni, M., Moore, H., Neukum, G., Schultz, P., Soderblom, L., Strom, R., Woronow, A., Young, R., 1979. Standard techniques for presentation and analysis of crater size-frequency data. Icarus 37, 467–474.

Breuer, D., Zhou, H., Yuen, D.A., Spohn, T., 1996. Phase transitions in the Martian mantle: implications for the planet's volcanic history. J. Geophys. Res. 101, 7531–7542. doi:10.1029/96JE00117.

Carr, M.H., 1974. Tectonism and volcanism of the Tharsis region of Mars. J. Geophys. Res. 79, 3943–3949.

Cheung, K.K., King, S.D., 2011. Using crustal thickness modeling to study Mars' crustal/mantle structures. 42nd Lunar Planet. Sci. Conf. Abstract, p. 1534.

Christensen, P.R., Jakosky, B.M., Kiefer, H.H., Malin, M.C., McSween Jr., H.Y., Nealson, K., Mehall, G.L., Silverman, S.H., Ferry, S., Caplinger, M., Ravine, M., 2004. The Thermal Emission Imaging System (THEMIS) for the Mars 2001 Odyssey Mission. Spa. Sci. Rev. 110, 85–130.

Connerney, J.E.P., Acuña, M.H., Wasilewski, P.J., Kletetschka, G., Ness, N.F., Rème, R.P., Mitchell, D.L., 2001. The global magnetic field of Mars and implications for crustal evolution. Geophys. Res. Lett. 28, 4015–4018.

Craddock, R.A., Howard, A.D., 2002. The case for rainfall on a warm, wet early Mars. J. Geophys. Res. 107. doi:10.1029/2001JE001505.

Dohm, J.M., Tanaka, K.L., 1999. Geology of the Thaumasia region, Mars: Plateau development valley origins, and magmatic evolution. Planet. Space Sci. 47, 411–431.

Dohm, J.M., Tanaka, K.L., Hare, T.M., 2001. Geologic map of the Thaumasia region of Mars. U.S. Geol. Surv. Misc. Invest. Map I–2650.

Frey, H.V., 1979. Thaumasia: a fossilized early forming Tharsis uplift. J. Geophys. Res. 84, 1009–1023.

Glen, J.M.G., Ponce, D.A., 2000. Large-scale fractures related to the inception of the Yellowstone hotspot. Geology 30, 647–650.

Greeley, R., Guest, J.E., 1987. Geologic map of the eastern equatorial region of Mars. U.S. Geol. Surv. Misc. Invest. Map I–1802–B.

Grimm, R.E., Solomon, S.C., 1986. Tectonic tests of proposed polar wander paths for Mars and the Moon. Icarus 65, 110–121.

Harder, H., Christensen, U.R., 1996. A one-plume model of Martian mantle convection. Nature 380, 507–509. doi:10.1038/380507a0.

Hartmann, W.K., 1999. Martian cratering VI: crater count isochrons and evidence for recent volcanism from Mars Global Surveyor. Meteorit. Planet. Sci. 34, 167–177.

Hartmann, W.K., Neukum, G., 2001. Cratering chronology and the evolution of Mars. Space Sci. Rev. 96, 165–194.

Head, J.W., Pratt, S., 2001. Extensive Hesperian-aged south polar ice sheet on Mars: evidence for massive melting and retreat, and lateral flow and ponding of meltwater. J. Geophys. Res. 106, 12275–12299.

Hood, L.L., Young, C.N., Richmond, N.C., Harrison, K.P., 2005. Modeling of major Martian magnetic anomalies: further evidence for polar reorientations during the Noachian. Icarus 177, 144–173.

Ivanov, B., 2001. Mars/Moon cratering rate ratio estimates. Chronology and Evolution of Mars. International Space Science Institute, Bern, pp. 87–104.

Johnson, C.L., Phillips, R.J., 2005. Evolution of the Tharsis region of Mars: insights from magnetic field observations. Earth Planet. Sci. Rev. 230, 241–254.

Kiefer, W.S., Hager, B.H., 1989. The role of mantle convection in the origin of the Tharsis and Elysium provinces of Mars. In: Frey, H. (Ed.), MEVTV Workshop on Early Tectonic and Volcanic Evolution of Mars. LPI Tech. Report 89–04, pp. 48–50.

Li, Q., Kiefer, W.S., 2007. Mantle convection and magma production on present-day Mars: effects of temperature-dependent rheology. Geophys. Res. Lett. 34. doi:10.1029/2007GL030544.

Lillis, R.J., Dufek, J., Bleacher, J.E., Manga, M., 2009. Demagnetization of crust by magmatic intrusion near the Arsia Mons volcano: magnetic and thermal implications for the development of the Tharsis province, Mars. J. Volcanol Geotherm. Res. 185, 123–138. doi:10.1016/j.jvolgeores.2008.12.007.

Lillis, R.J., Mitchell, D.L., Lin, R.P., Connerney, J.E.P., Acuña, M.H., 2004. Mapping crustal magnetic fields at Mars using electron reflectometry. Geophys. Res. Lett. 31. doi:10.1029/2004GL020189.

Matsuyama, I., Mitrovica, J.X., Manga, M., Perron, J.T., Richards, M.A., 2006. Rotational stability of dynamic planets with elastic lithospheres. J. Geophys. Res. 111. doi:10.1029/2005JE002447. E02003.

Mège, D., Masson, P., 1996. A plume tectonics model for the Tharsis province, Mars. Planet. Space Sci. 44, 1499–1546.

Melosh, H.J., 1980. Tectonic patterns on a reoriented planet—Mars. Icarus 44, 745–751.

Nimmo, F., Tanaka, K.L., 2005. Early crustal evolution of Mars. Annu. Rev. Earth Planet. Sci. 33, 133–161.

Perron, J.T., Mitrovica, J.X., Manga, M., Matsuyama, I., Richards, M.A., 2007. Evidence for an ancient Martian ocean in the topography of deformed shorelines. Nature 447, 840–843.

Phillips, R.J., Solomon, S.C., Zuber, M.T., Golombek, M.P., Jakosky, B.M., Banerdt, W.B., Smith, D.E., Williams, R.M.E., Hynek, B.M., Aharonson, O., Hauck II, S.A., 2001. Ancient geodynamics and global-scale hydrology on Mars. Science 291, 2587–2591.

Robbins, S.J., Di Achille, G., Hynek, B.M., 2010. The volcanic history of Mars: high-resolution crater-based studies of the calderas of twenty volcanoes. Icarus 211. doi:10.1016/j.icarus.2010.11.012.

Robbins, S.J., Hynek, B.M., 2010. A global Martian crater database complete to 1.5-km-diameter. 41st Lunar Planet. Sci. Conf. Abstract #2257.

Roberts, J.H., Zhong, S.J., 2007. The cause for the north-south orientation of the crustal dichotomy and the equatorial location of Tharsis on Mars. Icarus 190, 24–31.

Roberts, J.H., Zhong, S.J., 2004. Plume-induced topography and geoid anomalies and their implications for the Tharsis rise on Mars. J. Geophys. Res. 109, E03009. doi:10.1029/2003JE002226.

Singhal, B.B.B., 1997. Hydrogeological characteristics of the Deccan Trap formation in India. Hard Rock Hydrosystems IAHS Publ. no. 241.

Scott, D.H., Tanaka, K.L., 1986. Geologic map of the western equatorial region of Mars. U.S. Geol. Surv. Misc. Invest. Map I–1802–A.

Smith, D.E., Zuber, M.T., Frey, H.V., Garvin, J.B., Head, J.W., Muhleman, D.O., Pettengill, G.H., Phillips, R.J., Solomon, S.C., Zwally, H.J., Banerdt, W.B., Duxbury, T.C., Golombek, M.P., Lemoine, F.G., Neumann, G.A., Rowlands, D.D., Aharonson, O., Ford, P.G., Ivanov, A.B., McGovern, P.J., Abshire, J.B., Afzal, R.S., Sun, X., 2001. Mars Orbiter Laser Altimeter (MOLA): experiment summary after the first year of global mapping of Mars. J. Geophys. Res. 106, 23689–23722.

Solomon, S.C., Head, J.W., 1982. Evolution of the Tharsis province of Mars: the importance of heterogeneous lithospheric thickness and volcanic construction. J. Geophys. Res. 87, 9755–9774.

Šrámek, O., Zhong, S.J., 2010. Long-wavelength stagnant-lid convection with hemispheric variation in lithospheric thickness: link between Martian crustal dichotomy and Tharsis? J. Geophys. Res. doi:10.1029/2010JE003597.

Tanaka, K.L., Kolb, E.J., 2001. Geologic history of the polar regions of Mars based on Mars Global Surveyor Data: I. Noachian and Hesperian Periods. Icarus 154, 3–21.

Wenzel, M.J., Manga, M., Jellinek, A.M., 2004. Tharsis as a consequence of Mars' dichotomy and layered mantle. Geophys. Res. Lett. 31, L04702.

Whaler, K., Purucker, M., 2005. A spatially continuous magnetization model for Mars. J. Geophys. Res. 110, E09001. doi:10.1029/2004JE002393.

Willemann, R.J., 1984. Reorientation of planets with elastic lithospheres. Icarus 60, 701–709.

Zhong, S.J., 2009. Migration of Tharsis volcanism on Mars caused by differential rotation of the lithosphere. Nature Geosci. 2, 19–23.

Zuber, M.T., 2000. Internal structure and early thermal evolution of Mars from Mars Global Surveyor topography and gravity. Science 287, 1788–1793.